ANALYTICAL SCIENCES OCTOBER 2015, VOL. 31

Electrocatalytic Behavior of Hemoglobin Oxidation of Hydrazine Based on ZnO Nano-rods with Carbon Nanofiber Modified Electrode

Min Wu,† Wen Ding, Junli Meng, Henmei Ni,† Ying Li, and Quanhong Ma

School of Chemistry and Chemical Engineering, Southeast University, Nanjing 211189, P. R. China

A novel biosensor was developed by immobilizing hemoglobin (Hb) on a glassy carbon electrode (GCE) modified with a composite of ZnO nano-rods and carbon nanofiber (CNF), a strong reducer, hydrazine, was firstly used to evaluate the electrochemical behavior of Hb on Hb/ZnO/CNF/GCE. UV-vis and circular dichroism (CD) spectra indicated the conformational structure of Hb interaction with ZnO/CNF was predominantly an α-helical structure. The modified electrodes were characterized by scanning electron microscopy (SEM), electron impedance spectroscopy (EIS), and cyclic voltammetry. Electrocatalytic mechanism of Hb to oxidation reaction of hydrazine was suggested. The bioelectrocatalytic activity, kinetic parameters of Michaelis–Menten constant (K_m), stability and reproducibility were also investigated. A linear dependence of peak currents to the concentrations of hydrazine was observed in the range from 1.98×10^{-5} to 1.71×10^{-3} mol L^{-1} with a correlation coefficient of 0.998, and a detection limit (S/N = 3) of 6.60 μmol L^{-1} was estimated.

Keywords Nano-ZnO-carbon nanofiber, hydrazine, bio-electrocatalytic, hemoglobin

(Received April 15, 2015; Accepted June 15, 2015; Published October 10, 2015)

Introduction

Hydrazine is an important compound in the chemical and pharmaceutical industry. It sees not only widespread used in rocket fuels, missile systems, weapons of mass destruction and fuel cells,[1] but is also used as a catalyst, emulsifier, corrosion inhibitor and reducing agent. Hydrazine has been recognized as a neurotoxin, carcinogenic mutagenic and hepatotoxic substance, which threatens human health.[2] Therefore, quick and highly sensitive methods for the determination of hydrazine are required for environmental and biological analysis.[3] Numerous methods have been developed for the determination of hydrazine, such as chromatography,[4] spectrometry,[5,6] chemiluminescence,[7] flow injection analysis,[7,8] and electrochemical techniques.[9–12] Among them, in light of their fast response, high sensitivity, low cost, *etc.*,[13] the electrochemical techniques are considered to be relatively direct and effective for the detection of hydrazine. As an ideal model substance used for the fabrication of N_2H_4 biosensors, Hb is preferential for its known structure, ommercial availability and relatively high stability. However, a redox (hemoglobin (Hb))-based biosensor with high selectivity and specificity for N_2H_4 has not been reported yet. On the other hand, the oxidation of hydrazine is characterized by its irreversibility and large overvoltage at the bare carbon electrode. Therefore, various efforts have been made to chemically modify the carbon electrodes. Owing to the great progress in nanoscience and nanotechnology, it is possible to fabricate electrochemical sensors and biosensors for the determination of hydrazine by utilizing the unique properties of various nanostructures.[14]

As one of the nanoscale carbonaceous materials, carbon nanofiber (CNF) is well-known as an ideal substance for biosensors since it is conductive,[15] biocompatible, easily functionalized, and also offers a very large specific surface area.[16] With the cylindric nanostructure of the graphene layers that are arranged as stacked cones, cups, or plates, the mechanical strength and electric properties of CNF are similar to carbon nanotubes.[17] Moreover, the edge sites on the outer wall of CNF facilitate the electron transfer of electroactive analytes.[18] However, unfortunately since the closed shell of CNF is disadvantageous to a high degree of functionalization, the application of CNFs in biosensors is limited. Functionalization of CNFs is essential to the immobilization of biological molecules because the carbon atoms are chemically inert. Usually, oxidation[19] and chemical modification[20] are applied prior to modify the carbon nanofibers to be a biocompatible catalyst support. However, it is obvious that the oxidation and chemical modification are destructive to the carbon nanofibers, thereby interruptive to the electron transfer. Therefore, a new approach is necessary.

In addition to its high specific surface area, biocompatibility, chemical stability and non-toxicity, the nanostructured ZnO is attractive because of its biomimetic and high electron communication features,[21–22] and more importantly, a high isoelectric point (IEP) of about 9.5 as well. High IEP favors the nanostructured ZnO to adsorb the proteins with low IEPs because protein immobilization is primarily driven by electrostatic interaction. Additionally, ZnO with various nanostructures prepared by different fabrication techniques,

† To whom correspondence should be addressed.
E-mail: wuminnj@163.com (M. W.); Henmei_ni@hotmail.com (H. N.)

such as thermal decomposition,[22-23] hydrothermal,[24-25] and electrodeposition,[26] has been widely used for enzyme immobilization in recent years. It is reported that the electrochemical deposition is cost-effective, simple, and eco-friendly. These are the reasons why ZnO nanoparticles were selected in this paper.

The reversible redox reaction of $Fe^{II} \leftrightarrow Fe^{III}$ is readily performed in hemoglobin, thus an electrode adsorbing hemoglobin on its surface is a potential equipment for biosensing and electrocatalysis. Recent research focusing on the reduction of H_2O_2 with hemoglobin is likely due to the mimic motivation of hemoglobin action in blood. Researchers pay attention to the reducibility of Fe^{II} in hemoglobin to the substrates in most cases, while they place far less emphasis on the oxidizability of Fe^{III} to the substrate. In our preliminary study, utilizing the ability of triggering the reversible redox reaction, hemoglobin was explored as a biocatalyst to catalyze the oxidation of hydrazine. Hence, in this work, the strong reducer hydrazine will be used as the substrate and the biocatalysis of hemoglobin is investigated. We explored a novel way to fabricate the hydrazine biosensor. An Hb/ZnO/CNF composite membrane was prepared and applied for the bio-electrocatalytic oxidation of hydrazine. Without the addition of the electron transfer mediator, Oxidoreductase/ZnO/CNF modified electrode exhibited a fast response to hydrazine, which reflected high sensitivity of the direct electron transfer process between hydrazine and protein.

Experimental

Materials and reagents

CNF was provided by Beijing Science and Technology Co., Ltd. Shimadzu Deco. Hb was obtained from Aldrich. Zinc nitrate hexahydrate [$Zn(NO_3)_2{\cdot}6H_2O$] and potassium nitrate (KNO_3) were bought from Kelong Chemical's reagent plant in Chengdu. $N_2H_4{\cdot}H_2O$ (80%) and potassium hydroxide(KOH) were purchased from Sinopharm Chemical Reagent Co., Ltd. Phosphate-buffered saline (PBS, pH 7.0), which included 0.10 mol L^{-1} KCl, 0.10 mol L^{-1} K_2HPO_4 and 0.10 mol L^{-1} KH_2PO_4, was self-prepared. All of the chemicals used in this work were of analytical grade, and all of the solutions were prepared using doubly distilled water.

CNF was treated by acidification by nitric acid as described in the reference materials.[14,27] The obtained CNF functionalized with carboxylic groups was centrifuged at 3000*g* and washed completely with doubly distilled water. Then the homogeneous suspension of CNF was prepared by neutralizing the above solution to pH 7.0 after ultrasonic dispersion. It was stable for at least 3 months.

Preparation of ZnO/CNF composite membrane

The GCE was successively polished to a mirror finish using 1.0, 0.3 and 0.05 μm alumina slurry followed by rinsing thoroughly with water. After consecutive sonification in doubly distilled water, anhydrous ethanol and doubly distilled water, respectively, the GCE was finally rinsed with doubly distilled water and dried at room temperature.

The CNF/ GCE membrane was prepared by dropping CNF solution on the GCE and then dried with silica gel in a desiccator.

The CNF/GCE was shifted into an electrochemical cell containing 0.5 mM $Zn(NO_3)_2{\cdot}6H_2O$ and KNO_3 solution. The experiments were carried out in N_2 atmosphere. In total, 30 consecutive cyclic voltammograms were performed in the potential range between 0 and –1.5 V at a scanning rate of 50 mV s^{-1}. A ZnO/CNF nanocomposite membrane-modified electrode was prepared after the above electrode was rinsed with the doubly distilled water. It was stored in air prior to use.

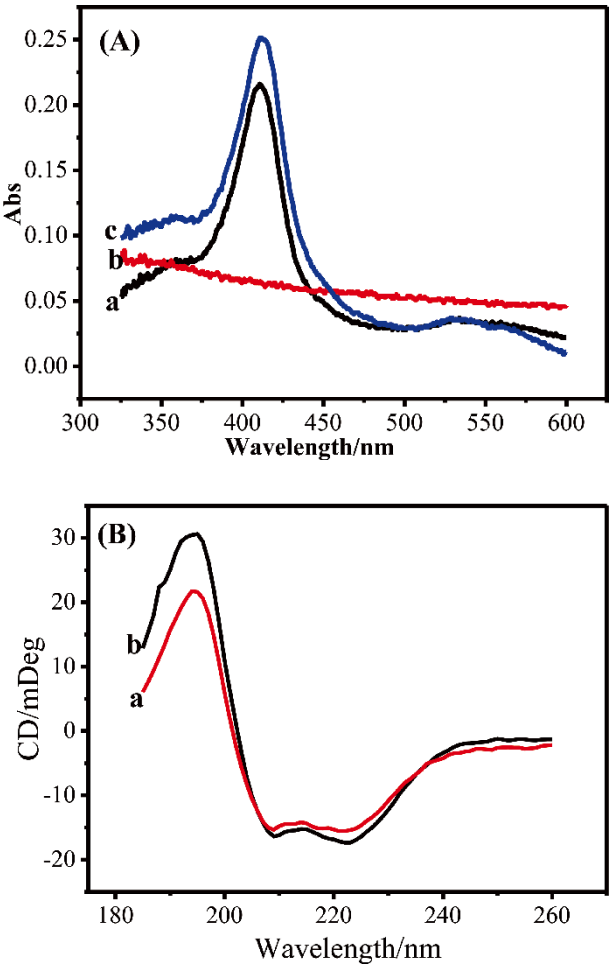

Fig. 1 P(A) UV-vis spectra of (a) Hb, (b) ZnO/CNF, (c) Hb/ZnO/CNF, (B) CD spectra of (a) Hb/ZnO/CNF, (b) Hb.

Preparation of Hb/ZnO/CNF/GCE

First, 6 μL of the Hb solution (10 mg mL^{-1} in 0.10 M phosphate buffer solution, pH 7.0) was coated on a ZnO/CNF/GCE, and then dried in the air. The achieved Hb/ZnO/CNF/GCE electrode was stored in a refrigerator (4°C) prior to use. For comparison, an Hb/CNF/GCE was also prepared by the same way.

Characterization

The surface images were taken by a scanning electron microscope (SEM) (Hitachi S-4800, Hitachi Co., Ltd., Tokyo, Japan). UV-vis spectroscopy was carried out in a spectrophotometer (UV-3600, Shimadzu Co., Ltd., Kyoto, Japan). The circular dichroism (CD) spectra of the samples were recorded by a German Bruker PMA50. A certain amount of CNF was cast on conductive glass slides, and then dried in the air. The Hb membrane was prepared by dispensing Hb on glass slides. ZnO/CNF and Hb/ZnO/CNF membranes were also prepared by the same way.

All electrochemical measurements were performed in the electrochemical analyzer (EC6100, Shanghai Sunny Hengping Scientific Instrument Co., Ltd., Shanghai, China) with a

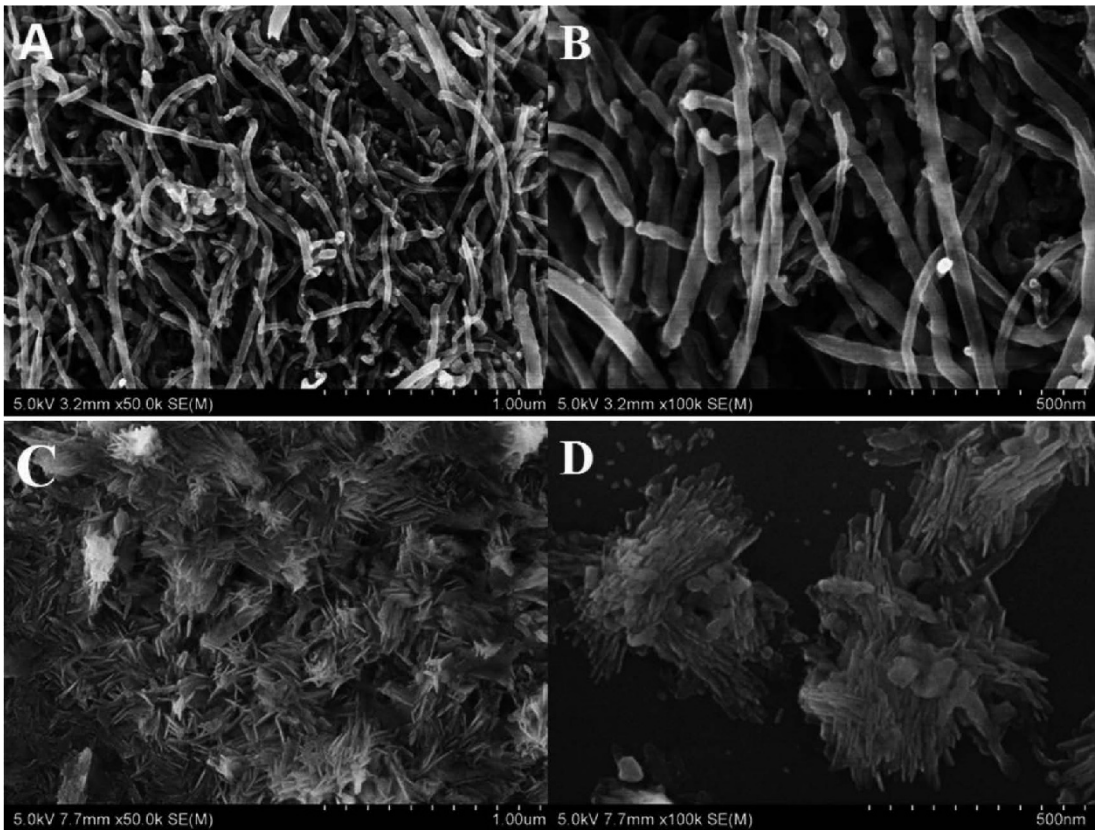

Fig. 2 SEM images of CNF/GCE (A, B) and ZnO/CNF/GCE (C, D).

conventional three-electrode system, *i.e.* a platinum wire as auxiliary electrode, a saturated calomel electrode (SCE) as reference, and a modified glassy carbon electrode (GCE, diameter 3.0 mm) as working electrode. A electrochemical workstation (Zahner IM6ex, Universal Analytical & Testing Instruments Ltd., Germany) (5.0 mV, 10^{-2} - 10^{5} Hz) was employed for the electrochemical impedance spectroscopy (EIS) where 5 mM $Fe(CN)_6^{3-}$/$Fe(CN)_6^{4-}$ (1/1, mol/mol) mixture with 0.10 M KCl was used as supporting electrolyte.

The step-wise increase of hydrazine concentration was carried out by continuously dripping the solution of hydrazine into the detecting system. The concentrations of hydrazine used for the dripping were 20 μM, 0.2 mM and 0.5 mM.

All experiments were performed at room temperature and in N_2 atmosphere.

Results and Discussion

Bioactivity of immobilized hemoglobin

As a biocatalyst, the structure of Hb plays a key role on its bio-activities. Hence, the first work of this paper is to confirm the structure of immobilized Hb. A normal and convenient approach reported is UV-Vis, namely that the shape and position of Soret absorption band of heme iron provides the valuable information of the denaturation of heme protein.[28,29] Therefore, UV-Vis was firstly employed for the detection of Hb/ZnO/CNF. The spectra including those of ZnO/CNF and Hb are shown in Fig. 1(A). As shown in Fig. 1(A), similar to that of the native Hb membrane (410 nm), the Soret band located at 411 nm was observed in the spectrum of Hb/ZnO/CNF. This result clearly suggested that the native structure of the Hb molecule was retained at the post-immobilization on ZnO/CNF, revealing the good biocompatibility of the composite matrix. Meanwhile, the conformational change of secondary structure of Hb in interaction with ZnO/CNF was employed by CD spectroscopy. As shown in Fig. 1(B), the positive peak was at 191 nm and two negative peaks were at 208 and 222 nm, which declare that Hb is an α-helix rich protein. The structure of Hb preserves its α-helical structure although the content of α-helix decreased slightly by adding ZnO/CNF. This implies that the bioactivity of Hb was not affected at the post-immobilization.

Surface morphologies of ZnO/CNF

Figure 2 shows the typical SEM images of the original CNF and CNF with the deposited ZnO at different magnifications. The surface morphology of the Hb/ZnO/CNF/GCE was indistinct. It was due to the poor conductivity of Hb. It was observed that the surface structure of CNF was greatly changed by the deposition of ZnO. For example, in contrast to the loose and porous texture of the original CNF (Figs. 2A and 2B), the surface of ZnO/CNF was fixed and solidified (Figs. 2C and 2D). CNF was covered by a mat consisting of nano-rods of ZnO crystal in the chemical process of deposition. The length of the ZnO nano-rods was around 80 to 100 nm. The diameter of the ZnO nano-rods was about 10 nm. (Fig. 2C). Moreover, in the SEM picture of broken pieces, the clear images of CNF were not observable (Fig. 2D). The clusters of ZnO nano-rods greatly enlarged the surface area of the ZnO/CNF composite, meanwhile the pI of ZnO was 9.5, thus the net positive surface charges on ZnO nano-rods were beneficial for immobilizing the negatively charged Hb.

As a result, SEM images indicated that high conductivity of CNF fibers were closely interconnected with porous ZnO nano-

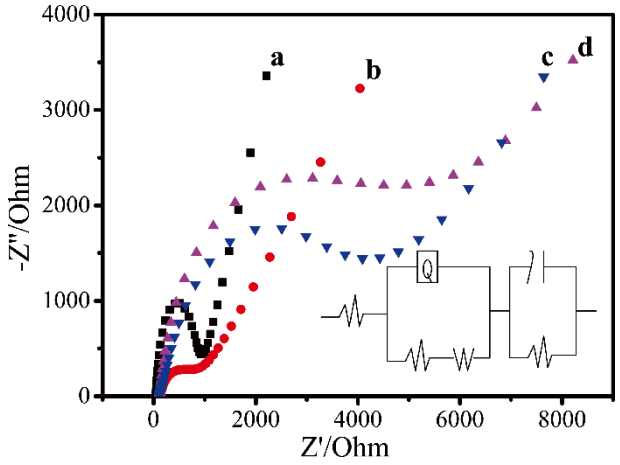

Fig. 3 Nyquist plots of 5.0 mM $[Fe(CN)_6]^{3-/4-}$ in 0.1 MKCl from 10 kHz to 0.1 Hz and Randles circuit model at open circle potential, obtained for (a) GCE, (b) CNF/GCE, (c) ZnO/CNF/GCE, (d) Hb/ZnO/CNF/GCE.

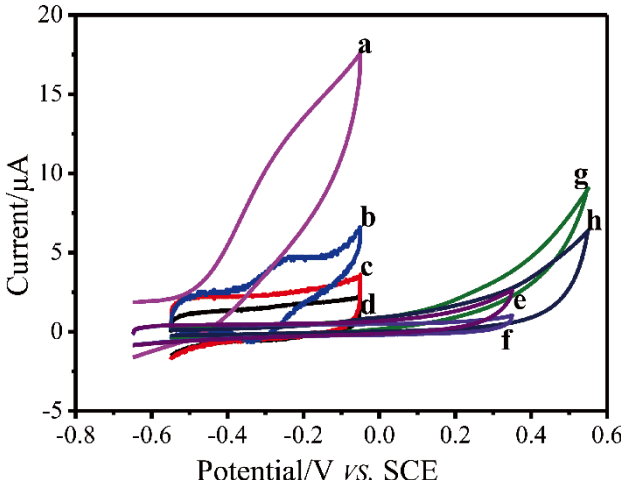

Fig. 4 Cyclic voltammograms (scanning rate, 20 mV^{-1}, pH 8.0) of GCE in the absence (f) and presence (e) of 1 mM hydrazine; CNF/GCE in the absence (h) and presence (g) of 1 mM hydrazine; ZnO/CNF/GCE in the absence (d) and presence (c) of 1 mM hydrazine; Hb/ZnO/CNF/GCE in the absence (b) and presence (a) of 1 mM hydrazine.

rods by chemical deposition. This microstructure was considered to reflect that both the enhanced absorption of bioactive Hb with large specific area of ZnO and electron transfer between N_2H_4 and the surface of Hb/ZnO/CNF/GCE.[30]

Electrochemical impedance of Hb/ZnO/CNF/GCE

The impedance changes of the electrode surface during the modification process were traced by electrochemical impedance spectroscopy (EIS). Electron transfer resistance (R_{et}) controls the electron transfer kinetics of the redox probe on the electrode surface and reflects the interfacial electron transfer ability, the value of which is estimated according to the diameter of semicircle of Nyquist plots at a high frequency region.[31] Accordingly, in the presence of Fe $(CN)_6^{3-}/Fe(CN)_6^{4-}$ (1:1) solution as supporting electrolyte at open circle potential about 0.225 V, the typical EIS were traced, corresponding to the bare GCE, CNF/GCE, ZnO/CNF/GCE and Hb/ZnO/CNF/GCE, respectively, and are shown in Fig. 3 along with the Randles circuit (inset) chosen for fitting the impedance data obtained in the experiments. As shown in Fig. 3, R_{et} values of bare GCE, CNF/GCE, ZnO/CNF/GCE and Hb/ZnO/CNF/GCE were estimated to be 432, 149.4, 2174 and 2470 Ω, respectively. It was expected that CNF/GCE would exhibit the lowest R_{et} because the high conductive CNF improved the performance of the electrode in the electron transfer between two ions, $Fe(CN)_6^{3-}$ and $Fe(CN)_6^{4-}$. Relatively, the conductance of ZnO is lower than CNF, thus ZnO/CNF/GCE gave the higher R_{et}, 2470 Ω. The higher Ret value of Hb/ZnO/CNF/GCE indicated that Hb molecules were successfully immobilized on the surface of ZnO/CNF/GCE and further resisted the electron transfer of the electrochemical probe.[32]

Electrocatalysis of Hb/ZnO/CNF/GCE to oxidation of hydrazine

Figure 4 shows the cyclic voltammograms (CVs) of modified GCE in 0.1 mol L^{-1} phosphate buffer solution (pH 7.0) with and without hydrazine with a scanning rate at 20 mV s^{-1}. A clear characteristic for all the CVs is that the background reduction currents are very faint. Moreover, as shown in Fig. 4, without ZnO, the oxidation currents are also faint irrespective of the existence of hydrazine. However, in the presence of ZnO, *i.e.* ZnO/CNF/GCE, the oxidation current is pronounced and further boosted by the existence of hydrazine. These results indicated that the electrode covered with ZnO nano-rods was more sensitive to the surrounding chemical change. Furthermore, in the presence of Hb, the situations were quite different. As shown in Fig. 4, there was a pair of characteristic peak currents observed on the CV of Hb/ZnO/CNF/GCE in the absence of hydrazine. These two peak currents were readily ascribed to the redox reaction of $Hb(Fe^{II}) \leftrightarrow Hb(Fe^{III})$. It indicated that a direct electron transfer between Hb and the electrode occurred. However, unlike those CVs of Hb modified electrode reported previously,[29] at first, the two potentials of redox reaction were positive. The formal potential (E^0), calculated from the average of oxidation and reduction peak potentials, was –0.285 V and the peak potential separation ($n\Delta E_p$) was approximately 100 mV, which was much larger than the theoretical value of reversible redox reaction, 59/n mV. Moreover, the reduction current including the peak current (i_{pa}) was very faint, but the background oxidation current was intense and increased with the increase of positive voltage. Additionally, the ratio of anionic and oxidation peak current, i_{pa}/i_{pc} = 0.52/4.75, was much smaller than 1. The larger separation of peak potentials and smaller ratio of peak currents are the criteria of quasi-reversible redox reaction process. Hence, it indicated that the electrochemistry of Hb/ZnO/CNF/GCE was so quasi-reversible as to near the irreversible.

In the solution of hydrazine, a special phenomenon was observed on the CV of Hb/ZnO/CNF/GCE. As shown in Fig. 4, the characteristic reduction current peak completely disappeared corresponding to the $Hb(Fe^{III})$ reduction. Instead, only the peak current corresponding to the oxidation of $Hb(Fe^{II})$ was observed accompanying a strong oxidation background current. It indicated that only the oxidation of $Hb(Fe^{II})$ occurred on the electrode in the presence of hydrazine, whilst the reduction of $Hb(Fe^{III})$ took place beyond the electrode surface.

In order to further confirm the above observations, the effect of scanning rate on the cyclic voltammogram of Hb/ZnO/CNF/GCE was investigated in the rate range of 10 - 200 mV s^{-1}. As shown in Fig. S1A (Supporting Information), it is obvious that the characteristic cyclic voltammogram was reproduced at various scanning rates in the presence of 1.0 mM N_2H_4. Moreover, the peak current increased as the scanning rate

increased. On the other hand, the relationship between oxidation currents and scanning rate was evaluated. As shown in Fig. S1B (Supporting Information), it was observed that the oxidation currents were positively proportional to the square root of scanning rate (I_p (μA) = 8.91 + 2.40 $\sqrt{v}$ (R_2 = 0.998)). It is coincident to the theoretical predication of the diffusion-controlled process.

Based on all the above results, the following catalytic mechanism (EC catalytic mechanism[33,34]) was suggested to describe the oxidation of hydrazine in the presence of Hb/ZnO/CNF.

On the electrode:

$$2Hb[(Heme)Fe^{II}] \rightarrow 2Hb[(Heme)Fe^{III}] + 2H^+ + 2e^- \quad (1)$$

In the solution:

$$2Hb[(Heme)Fe^{III}] + 2N_2H_5OH \rightarrow N_2 + 2NH_3 + 2H_2O + 2Hb[(Heme)Fe^{II}] \quad (2)$$

Total reaction:

$$2N_2H_4 + 2OH^- \rightarrow N_2 + 2NH_3 + 2H_2O \quad (3)$$

That is to say, the reduction reaction of (heme) Fe^{III} took place in the solution of hydrazine, thus the reduction current peak was not observed in the cyclic voltammogram (Fig. 4). Only the oxidation reaction of $Fe^{II} \rightarrow Fe^{III}$ occurred on the electrode.

Figure S1C (Supporting Information) shows the magnitudes of peak potential *vs.* logarithm of scanning rates. It was clear that E_p was proportional to the logarithm of scanning rate. According to this plot, the charge transfer coefficient, α, and the number of electrons, n_α, transferred between hydrazine and Hb[(Heme)Fe^{II} were assessable. Tafel slope, b, was obtained from the linear relationship of E_p *vs.* log (v) by using the following equation, where v was the scanning rate and c, a constant.

$$E_p = \frac{b}{2}\log(v) + c \quad (4)$$

Hence, according to the simulated result shown in Fig. S1C (Supporting Information),

$$Y = 0.0769X + 0.00149. \quad (5)$$

It was obtained that b = 154 mV decade^{-1}. Moreover, as we know,

$$b = \frac{2.3RT}{(1-\alpha)n_\alpha F} \quad (6)$$

where R is the gas constant, T the absolute temperature and F the Faraday constant. Therefore, $(1 - \alpha)n_\alpha = 0.38$. For most electrode processes, n_α was an integral number and α ranged from 0.25 to 0.75.[12] Accordingly, $\alpha = 0.62$ was rational, by which $n_\alpha = 1$. That is to say, the process of oxidation was consistent to one electron transfer process in the rate-determining step.

Sensitivity of Hb/ZnO/CNF/GCE

Sensitivity of Hb/ZnO/CNF/GCE towards the oxidation of N_2H_4 was investigated with CV and amperometry, accompanying the drop-wise addition of hydrazine. As shown in Fig. S3 (Supporting Information), the sensitivity of cyclic voltammetry

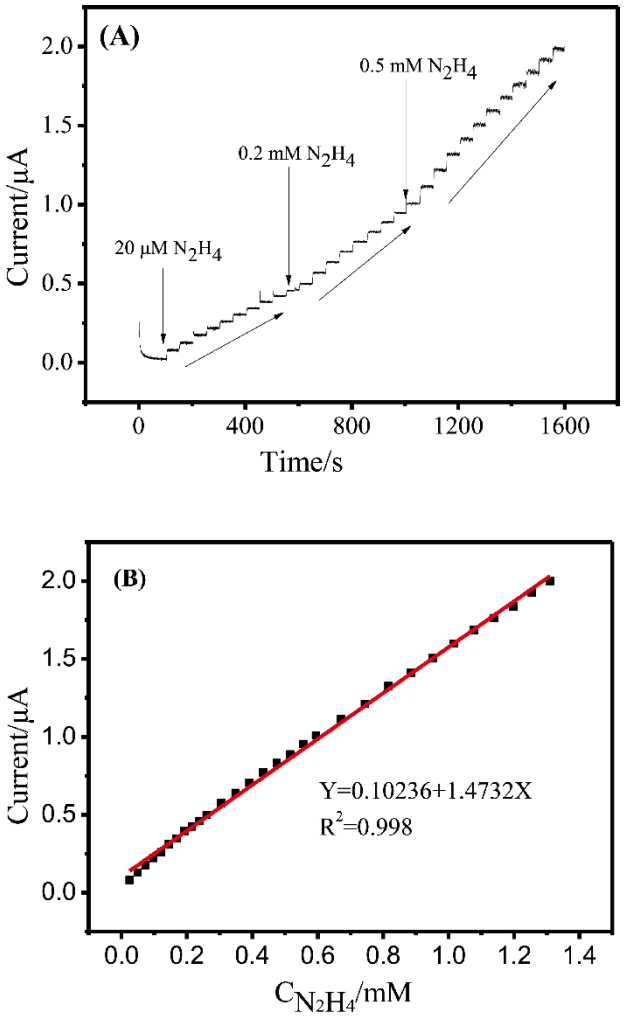

Fig. 5 Sensitivity of Hb/ZnO/CNF/GCE to the concentration of hydrazine ((A) current *vs.* time curves with step-wise addition of hydrazine at pH 7.0, (B) calibration curves for hydrazine, operating potential: 0.40 V).

was substantially limited at low concentrations, thus amperometry was further employed. Figure 5 shows a typical hydrodynamic amperometric response obtained at a constant potential of 0.4 V by consecutively adding hydrazine (0.1 M PBS, pH 7.0). As shown in Fig. 5A, with the step-wise increase of N_2H_4 concentration, the step-wise response was observed. Moreover, corresponding to each run of adding N_2H_4, it took less than 5 s for the current to reach 96% of its maximum value. This result further confirmed that Hb/ZnO/CNF/GCE was very sensitive to the variation of hydrazine concentrations. The current response *vs.* N_2H_4 concentration is shown in Fig. 5B. It indicated that the current was linearly correlated to the concentration of hydrazine over a wide span of as much as 1.98×10^{-2} – 1.71 mM. By this plot, the detecting limit of Hb/ZnO/CNF/GCE was evaluated to be 6.60 μM corresponding to the ratio of signal-to-noise (S/N) = 3. As comparisons, the larger spans of measurable concentration and the lower detecting limits of some other modified electrodes reported[10,11,38] in the references specially developed for the detection of hydrazine are listed in Table 1. Some detection limits of those modified electrodes were high[10] and some linear ranges were narrow.[11,35] As shown in Table 1, the comprehensive performance of Hb/ZnO/CNF/GCE was the appropriate for the detection of

Table 1 Electroanalytical characteristics of various modified electrodes for N_2H_4 detection

Modified electrode	pH (solution)	Linear range/ μmol L^{-1}	Detecting limit/ μmol L^{-1}	Ref.
Co(II)BBAEDI-MWCNF-MCPE	7.0	0.3 – 70	0.10	10
NiHCF/CC	7.0	20 – 2000	8.00	11
Lu/MWNT-IL/SPCE	7.0	0.02 – 120	0.0066	35
Hb/ZnO/CNF/GCE	8.0	19.8 – 1710	6.60	Present paper

hydrazine.

On the other hand, the current deviated from linearity and leveled off when the concentration of N_2H_4 was higher than 1.71 mM, which showed the characteristics of the apparent Michaelis–Menten kinetics. Therefore, the apparent Michaelis–Menten constant (K_M^{app}) was obtained according to the Lineweaver–Burk equation,

$$\frac{1}{I_{ss}} = \frac{1}{I_{max}} + \frac{K_M^{app}}{I_{max}C} \quad (7)$$

where I_{ss} was the current of steady-state after the addition of substrate, C the bulk concentration of substrate and I_{max} the maximum current in the saturated solution of substrate. We found K_M^{app} = 1.08 mmol L^{-1}, which was much lower than those in some other reporteds.[35-37] The lower value of K_M^{app} represented a higher biological affinity of Hb in the catalytic reaction of N_2H_4.

Interference studies

The interference experiment was studied under optimum conditions and a standard solution of 5.0×10^{-4} M hydrazine was used. The interference cations and anions were Na^+, K^+, NH_4^+, Ca^{2+}, Mg^{2+}, F^-, Cl^-, Br^-, I^-, NO_3^- SO_4^{2-}, CO_3^{2-}, PO_4^{3-}, CH_3COO^-, $C_2O_4^{2-}$, glucose, lactose, and fructose, with 100, 500, 1000-fold of hydrazine in quantities. The experiment results showed that, the deviation of the determination of hydrazine was within 4.3%. It did not obviously interfere with the determination of hydrazine.

Reproducibility and stability of Hb/ZnO/CNF/GCE

The stability and reproducibility of Hb/ZnO/CNF/GCE were examined by cyclic voltammetry. The relative standard deviation (RSD) was less than 3.27% in the continuous eight cycles of measurements with 1.0 mmol L^{-1} N_2H_4 in PBS. The current of oxidation peaks exhibited no significant change after 20 cycles. After 20 cycles, it retained almost 95% of its initial value. It demonstrated that the performance of Hb/ZnO/CNF/GCE was reproducible. The stability of Hb/ZnO/CNF/GCE in storage was examined by storing the same electrodes at 4°C for 2 weeks, and 2 weeks later, the oxidation peak current generally retained above 97%. These results indicated that the biosensor based on Hb/ZnO/CNF/GCE exhibited good stability and reproducibility.

Conclusions

A sensitive hydrazine biosensor was developed by immobilizing Hb on a glassy carbon electrode (GCE) modified with ZnO nano-rods electrochemically deposited on carbon nanofiber. By UV-vis and CD spectra, it was confirmed that the native structure of Hb was retained in the post-immobilization on ZnO/CNF. SEM and EIS results indicated that the composite of CNF and ZnO nano-rods allowed the electrons to freely transfer on the electrodes. The porous ZnO nano-rods provided a large specific area and good biocompatibility for the immobilization of Hb. Electrocatalytic mechanism of Hb to the oxidation of hydrazine was suggested. The oxidation process for hydrazine that occurred on the Hb/ZnO/CNF/GCE electrode was a one electron transfer in the rate-determining step.The bioelectrocatalytic activity was also investigated. The apparent Michaelis–Menten constant (K_M^{app}) of hydrazine oxidation was evaluated to be 1.08 mmol L^{-1}, representing a higher biological affinity of Hb in the catalytic reaction of hydrazine. A linear dependence of peak currents to the concentrations of hydrazine was observed in the range from 1.98×10^{-5} to 1.71×10^{-3} mol L^{-1} with a correlation coefficient 0.998, and a detection limit (S/N = 3) of 6.60 μmol L^{-1} was estimated. Hb/ZnO/CNF/GCE exhibited good sensitivity, stability and reproducibility for the detection of hydrazine.

Acknowledgements

The authors acknowledge financial assistance from the National Natural Science Foundation of China (NSFC, Grant No. 21005016), Educational Commission of Jiangsu Province (No. JHB2011-2). This paper was reviewed and revised by Prof. Henmei Ni.

Supporting Information

Support materials mainly describes that Hb/ZnO/CNF test the hydrazine effected by the sweep speed, pH, different concentration of hydrazine. This material is available free of charge on the Web at http://www.jsac.or.jp/analsci/.

References

1. A. Abbaspour, A. Khajehzadeh, and A. Ghaffarinejad, *J. Electroanal., Chem.*, **2009**, *631*, 52.
2. B. Fang, Y. Feng, M. Liu, G. Wang, X. Zhang, and M. Wang, *Microchim., Acta*, **2011**, *175*, 145.
3. H. R. Zare and N. Nasirizadeh, *Electroanalysis*, **2006**, *18*, 507.
4. R. Gilbert and R. Rioux, *Anal. Chem.*, **1984**, *56*, 106.
5. J. A. Oh, J. H. Park, and H. S. Shin, *Anal. Chim. Acta*, **2013**, *769*, 79.
6. M. George, K. S. Nagaraja, and N. Balasubramanian, *Talanta*, **2008**, *75*, 27.
7. A. Safavi and M. A. Karim, *Talanta*, **2002**, *58*, 785.
8. A. A. Ensafi and M. A. Chamjangali, *J. Anal. Chem.*, **2004**, *59*, 129.
9. C. Tan, X. Xu, F. Wang, Z. Li, J. Liu, and J. Ji, *Sci. China Chem.*, **2013**, *56*, 911.
10. C. d. D. C. Conceição, R. C. Faria, O. Fatibello-Filho, and A. A. Tanaka, *Anal. Lett.*, **2008**, *41*, 1010.
11. A. Benvidi, P. Kakoolaki, H. R. Zare, and R. Vafazadeh, *Electrochim. Acta*, **2011**, *56*, 2045.
12. M. A. Kamyabi, O. Narimani, and H. H. Monfared, *J. Electroanal. Chem.*, **2010**, *644*, 67.
13. J. Li and X. Lin, *Sens. Actuators, B*, **2007**, *126*, 527.
14. L. N. Wu, X. J. Zhang, and H. X. Ju, *Anal. Chem.*, **2007**, *79*, 453.

15. N. M. Rodriguez, M. S. Kim, and R. T. K. Baker, *J. Phys. Chem.*, **1994**, *98*, 13108.
16. V. Vamvakaki, K. Tsagaraki, and N. Chaniotakis, *Anal. Chem.*, **2006**, *78*, 5538.
17. M. Endo, Y. A. Kim, T. Hayashi, Y. Fukai, and K. Oshida, *Appl. Phys. Lett.*, **2002**, *80*, 1267.
18. B. N. Wu, C. Y. Hu, X. Q. Hu, H. M. Cao, C. S. Huang, H. B. Shen, and N. Q. Jia, *Biosens. Bioelectron.*, **2013**, *50*, 300.
19. B. R. Azamian, K. S. Coleman, J. J. Davis, N. Hanson, and M. L. H. Green, *Chem. Commun.*, **2002**, *4*, 366.
20. V. Vamvakaki, M. Hatzimarinaki, and N. Chaniotakis, *Anal. Chem.*, **2008**, *80*, 5970.
21. Z. R. Tian, J. A. Voigt, J. Liu, B. Mckenzie, and M. J. Mcdermott, *J. Am. Chem. Soc.*, **2002**, *124*, 12954.
22. Y. T. Wang, L. Yu, J. Wang, L. Lou, W. J. Du, Z. Q. Zhu, H. Peng, and J. Z. Zhu, *J. Electroanal. Chem.*, **2011**, *661*, 8.
23. J. Liu, C. Guo, C. M. Li, Y. Li, Q. Chi, X. Huang, L. Liao, and T. Yu, *Electrochem. Commun.*, **2009**, *11*, 202.
24. R. Ahmad, N. Tripathy, and Y. B. Hahn, *Sens. Actuators, B*, **2012**, *169*, 382.
25. B. X. Gu, C. X. Xu, G. P. Zhu, S. Q. Liu, L. Y. Chen, M. L. Wang, and J. J. Zhu, *J. Phys. Chem. B*, **2009**, *113*, 6553.
26. Y. L. Chen, Z. A. Hu, Y. Q. Chang, H. W. Wang, Z. Y. Zhang, Y. Y. Yang, and H. Y. Wu, *J. Phys. Chem. C*, **2011**, *115*, 2563.
27. C. Hao, L. Ding, X. J. Zhang, and H. X. Ju, *Anal. Chem.*, **2007**, *79*, 4442.
28. P. George and G. Hanania, *Biochem. J.*, **1953**, *55*, 236.
29. S. Palanisamy, S. Cheemalapati, and S. M. Chen, *Anal. Biochem.*, **2012**, *429*, 108.
30. C. Park and R. T. K. Baker, *J. Phys. Chem. B*, **1998**, *102*, 5168.
31. H. Wang, X. Bo, J. Ju, and L. Guo, *Catal. Sci. Technol.*, **2012**, *2*, 2327.
32. F. Chekin, J. B. Raoof, S. Bagheri, and S. B. A. Hamid, *Anal. Methods*, **2012**, *4*, 2977.
33. S. M. Golabi and H. R. Zare, *J. Electroanal. Chem.*, **1999**, *465*, 168.
34. H. M. Nassef, A. E. Radi, and C. K. O'Sullivan, *J. Electroanal. Chem.*, **2006**, *592*, 139.
35. S. H. Wu, F. H. Nie, Q. Z. Chen, and J. J. Sun, *Anal. Methods*, **2010**, *2*, 1729.
36. A. Senthil Kumar, P. Gayathri, P. Barathi, and R. Vijayaraghavan, *J. Phys. Chem.*, **2012**, *116*, 23692.
37. M. Wu, Q. He, Q. F. Shao, Y. G. Wang, F. Zuo, and H. M. Ni, *ACS Appl. Mater. Interfaces*, **2011**, *3*, 3300.